



HAL
open science

Transmorphic epitaxial growth of AlN nucleation layers on SiC substrates for high-breakdown thin GaN transistors

Jun Lu, Jr-Tai Chen, Martin Dahlqvist, Riad Kabouche, F Medjdoub, Johanna Rosen, Olof Kordina, Lars Hultman

► To cite this version:

Jun Lu, Jr-Tai Chen, Martin Dahlqvist, Riad Kabouche, F Medjdoub, et al.. Transmorphic epitaxial growth of AlN nucleation layers on SiC substrates for high-breakdown thin GaN transistors. Applied Physics Letters, 2019, 115 (22), pp.221601. 10.1063/1.5123374 . hal-02400602

HAL Id: hal-02400602

<https://hal.science/hal-02400602v1>

Submitted on 2 Dec 2020

HAL is a multi-disciplinary open access archive for the deposit and dissemination of scientific research documents, whether they are published or not. The documents may come from teaching and research institutions in France or abroad, or from public or private research centers.

L'archive ouverte pluridisciplinaire **HAL**, est destinée au dépôt et à la diffusion de documents scientifiques de niveau recherche, publiés ou non, émanant des établissements d'enseignement et de recherche français ou étrangers, des laboratoires publics ou privés.


Transmorphic epitaxial growth of AlN nucleation layers on SiC substrates for high-breakdown thin GaN transistors

Cite as: Appl. Phys. Lett. **115**, 221601 (2019); <https://doi.org/10.1063/1.5123374>

Submitted: 05 August 2019 . Accepted: 22 October 2019 . Published Online: 25 November 2019

Jun Lu, Jr-Tai Chen , Martin Dahlgqvist, Riad Kabouche, Farid Medjdoub, Johanna Rosen, Olof Kordina, and Lars Hultman 

COLLECTIONS

 This paper was selected as Featured



View Online



Export Citation



CrossMark

ARTICLES YOU MAY BE INTERESTED IN

[A GaN-SiC hybrid material for high-frequency and power electronics](#)

Applied Physics Letters **113**, 041605 (2018); <https://doi.org/10.1063/1.5042049>

[Reduced dislocation density and residual tension in AlN grown on SiC by metalorganic chemical vapor deposition](#)

Applied Physics Letters **115**, 161101 (2019); <https://doi.org/10.1063/1.5123623>

[Boosting the doping efficiency of Mg in p-GaN grown on the free-standing GaN substrates](#)

Applied Physics Letters **115**, 172103 (2019); <https://doi.org/10.1063/1.5124904>

Lock-in Amplifiers

... and more, from DC to 600 MHz



Transmorphic epitaxial growth of AlN nucleation layers on SiC substrates for high-breakdown thin GaN transistors

Cite as: Appl. Phys. Lett. **115**, 221601 (2019); doi: [10.1063/1.5123374](https://doi.org/10.1063/1.5123374)

Submitted: 5 August 2019 · Accepted: 22 October 2019 ·

Published Online: 25 November 2019



View Online



Export Citation



CrossMark

Jun Lu,^{1,a)} Jr-Tai Chen,^{2,a)}  Martin Dahlqvist,¹ Riad Kabouche,³ Farid Medjdoub,³ Johanna Rosen,¹ Olof Kordina,² and Lars Hultman¹ 

AFFILIATIONS

¹Thin Film Physics Division, Department of Physics (IFM), Linköping University, SE-581 83 Linköping, Sweden

²SweGaN AB, Teknikringen 8D, SE-583 30 Linköping, Sweden

³Institute of Electronic, Microelectronic and Nanotechnology, Av. Poincaré, 59650 Villeneuve d'Ascq, France

^{a)}Electronic addresses: jun.lu@liu.se and jr-tai.chen@swegan.se

ABSTRACT

Interfaces containing misfit dislocations deteriorate electronic properties of heteroepitaxial wide bandgap III-nitride semiconductors grown on foreign substrates, as a result of lattice and thermal expansion mismatches and incompatible chemical bonding. We report grain-boundary-free AlN nucleation layers (NLs) grown by metalorganic chemical vapor deposition on SiC (0001) substrates mediated by an interface extending over two atomic layers L1 and L2 with composition $(\text{Al}_{1/3}\text{Si}_{2/3})_{2/3}\text{N}$ and $(\text{Al}_{2/3}\text{Si}_{1/3})\text{N}$, respectively. It is remarkable that the interfaces have ordered vacancies on one-third of the Al/Si position in L1, as shown here by analytical scanning transmission electron microscopy and *ab initio* calculations. This unique interface is coined the out-of-plane compositional-gradient with in-plane vacancy-ordering and can perfectly transform the in-plane lattice atomic configuration from the SiC substrate to the AlN NL within 1 nm thick transition. This transmorphic epitaxial scheme enables a critical breakdown field of ~ 2 MV/cm achieved in thin GaN-based transistor heterostructures grown on top. Lateral breakdown voltages of 900 V and 1800 V are demonstrated at contact distances of 5 and 20 μm , respectively, and the vertical breakdown voltage is ≥ 3 kV. These results suggest that the transmorphic epitaxially grown AlN layer on SiC may become the next paradigm for GaN power electronics.

© 2019 Author(s). All article content, except where otherwise noted, is licensed under a Creative Commons Attribution (CC BY) license (<http://creativecommons.org/licenses/by/4.0/>). <https://doi.org/10.1063/1.5123374>

Epitaxial thin films are the fundamental element in solid-state electronics, for which the interface determines the layer quality. However, growth of a heteroepitaxial single-crystal film with a low defect density is difficult because of the inevitable lattice, thermal expansion mismatches, and chemical composition incompatibility between the film and the substrate, which induce dislocations, pits, or grain boundaries.^{1–3} Since the heteroepitaxy of GaN layers was invented in 1986 by Amano *et al.* using an AlN layer,⁴ AlN has been commonly used as a nucleation layer (NL) to facilitate two-dimensional growth of the GaN layers for wide-range applications, from optoelectronics as light-emitting and laser diodes to high-power devices as high electron mobility transistors (HEMTs). Nevertheless, the issue of high-density dislocations in GaN layers remains daunting as they degrade the breakdown characteristic. Typically, the critical breakdown field of lateral GaN HEMTs grown on foreign substrates, like sapphire, Si, and SiC, can only reach values in a range of 0.6–0.85 MV/cm, which is far below

the ultimate theoretical value of 3 MV/cm.⁵ Therefore, to fully unlock the potential of the GaN devices, the dislocation density in the GaN layers has to be minimized, where the most relevant place to suppress the formation of structural defects in the epitaxial layers may lie in the very first interface, i.e., the one between the AlN NL and the substrate. Any defects like pits and dislocations starting to form at this interface would require extra efforts to be annihilated. Inevitably, the inefficient approach of increasing the thickness of the epitaxial layers and/or increasing the number of intermediate layers often has to be employed to alleviate this issue.⁶

Here, we reveal an out-of-plane compositional-gradient with an in-plane vacancy-ordering (opCG-ipVO) interface structure formed in between an AlN NL and a SiC substrate from a sample (A) consisting of a high-quality thin GaN HEMT heterostructure⁷ and compare it with a reference (B) that contains the same heterostructure, but with a commonplace AlN/SiC abrupt interface without in-plane vacancy

ordering. The thickness of the AlN NLs is in a range of 15–60 nm in this study. Samples A and B with the thin GaN HEMT heterostructure were grown by a metalorganic chemical vapor deposition (MOCVD) system on 4H semi-insulating SiC substrates by SweGaN AB. High-purity NH_3 , TMAI, and TMGa were used as the precursors for the growth of III-nitride epitaxial layers with a mixture of N_2 and H_2 as carrier gases. The growth of samples A and B was based on the conditions described in Ref. 7, where the low-thermal-boundary-resistance (TBR) AlN NL and the conventional AlN NL are used in the thin GaN HEMT heterostructures. Moreover, the crystalline quality of the AlN NL and the thin GaN channel layer of sample A, assessed by X-ray diffraction rocking curves (XRC), is on a par with the quality shown in Ref. 7. However, the full width at half maximum (FWHM) values of XRC for the (002) reflections of the AlN NL and the GaN channel layer in sample B are much higher than those of sample A, which are 315 and 607 arc sec, respectively. Cross-sectional TEM specimens were prepared by an established method.⁸ High-resolution analytical scanning transmission electron microscopy (STEM) operated with high angle annular dark field (HAADF) and super-X energy dispersive spectroscopy (EDX) detectors in combination with *ab initio* calculations is used to characterize the interface structures. Z-contrast images⁹ and EDX mappings were acquired by using the double-corrected Linköping FEI Titan3 60–300 operated at 300 kV with a resolution of 0.7 Å.

Overviews of the samples in the region of GaN/AlN/SiC are shown in Figs. 1(a) and 1(b). Sample A, shown in Fig. 1(a), has a high structural quality that exhibits a low threading dislocation density, grain-boundary-free AlN NL, and atomically flat GaN/AlN/SiC interfaces. The bright contrast with a spacing of ~ 10 nm along the GaN/AlN interface is caused by localized stress fields from the misfit dislocations. In contrast, in sample B, the surface of the AlN NL is rough, with a number of pits. As seen in the TEM images, most of the dislocations in the AlN NL are generated at the AlN/SiC interface and then penetrate the AlN NL, propagating into the GaN layer. Obviously, the AlN/SiC interface plays a critical role in the quality of the epitaxial AlN layer and GaN layer.

Figures 1(c) and 1(d) show the AlN/SiC interfaces of samples A and B, oriented along $[1\bar{1}00]$, which confirm large structural differences between the two samples. Sample A has an atomically flat in-plane ordered AlN/SiC interface, shown in Fig. 1(c), which consists of two intermediate layers, viz., the first and the second intermediate layer. Such a step-free interface structure continuously extends over several hundred nanometers (as shown in Fig. S1) until reaching a SiC atomic surface step. The sparse surface steps are naturally generated because of a 0.1° cutoff angle from the on-axis for the SiC substrate used here. In contrast, sample B has an AlN/SiC interface without in-plane ordering. Regular surface steps are observed within a few tens of nanometers range [see Fig. 1(d)] along the interface. These steps are responsible for the creation of threading dislocations at the AlN/SiC interface.¹⁰ Clearly, the long-range step-free opCG-ipVO interface provides a unique foundation that is capable of suppressing the defect formation in the beginning of the heteroepitaxy of AlN on the SiC substrate.

The corresponding EDX mapping displayed in Fig. 1(f) pinpoints the chemical composition of sample A. Figure 1(e, left) exhibits a clear interface, above which is a 2H structure suggesting an AlN layer and below is a 4H structure indicating the SiC substrate. However, the EDX measurement shows a more complex ordered chemistry across

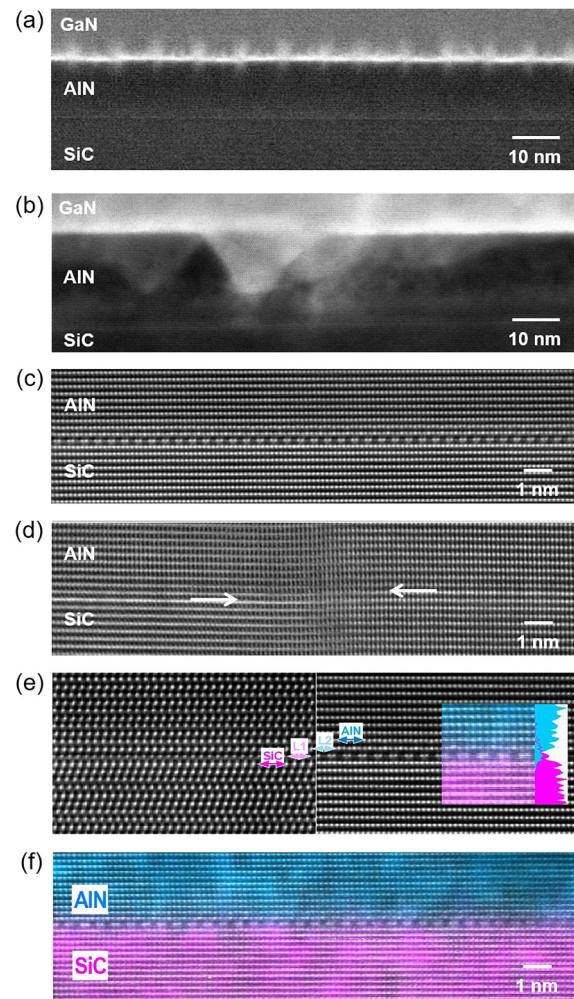


FIG. 1. Cross-sectional TEM overview images of sample A (a) and sample B (b) along $[1\bar{1}20]$. Cross-sectional STEM images of AlN/SiC interfaces, sample A (c), and sample B (d) along the $[10\bar{1}0]$ zone axis. Z-contrast images and EDX mapping of sample A in (e) and (f). STEM image along $[11\bar{2}0]$ (e, left) and STEM image along $[10\bar{1}0]$ (e, right) and the corresponding EDX mapping along $[10\bar{1}0]$ (f). The inset in (e, right) shows an enlarged EDX map and the EDX line scan. The first layers of the film and the substrate adjacent to L2 and L1 are labeled by AlN in blue and SiC in pink.

the interface. The first layer of the 2H structure marked as L1 contains not only Al and N but also Si with approximately two times higher content than for Al. In the Z-contrast STEM image, C and N are too light to give discernible contrast, while Al and Si are too close in the atomic mass, resulting in similar Z contrast, and hence are not easily distinguishable. The low contrast of L1 implies a substantial fraction of vacancies, and a STEM image observed from $[10\bar{1}0]$ orientation shows in-plane ordering [see Fig. 1(e, right)]. The bright pairs have almost the same intensity as that of Al or Si, while the position between them is of low intensity, clearly exhibiting partial vacancy formation. The composition of L1 with a high Si content implies that L1 is not the first layer of the AlN, but an intermediate layer. The layer above the L1 also contains Al, N, and Si, with an Al/Si ratio of 2:1, indicating the second

intermediate layer, viz., L2. L2 also displays an in-plane ordered structure but with an opposite intensity distribution in the Z-contrast STEM image [see Fig. 1(e, right)]. In a likelihood, the positions with high bright contrast have high occupancy, while the pairs of reduced intensity imply a lower occupancy. The layers above L2 or below L1 also contain traces of Si or Al, as shown by the composition line scan profile in the inset in Fig. 1(e, right).

Figures 2(a)–2(f) show a STEM image along $[10\bar{1}0]$ and the corresponding structure model together with a series of schematics displaying the basal layers of AlN, SiC, and the 2D networks of L1 and L2. For brevity, only Al (in blue) and Si (in pink) atoms are exhibited in Fig. 2 without showing C and N (which have weak or vanishing contrast in STEM). The first AlN and the SiC basal-plane layers (L3 and L0) are illustrated in Figs. 2(c) and 2(f), respectively. Between them are the two intermediate layers L2 and L1, as shown in Figs. 2(d) and 2(e), respectively. As mentioned, L1 is constituted by Si and Al in a 2:1 ratio, from EDX measurements, and N. Based on the experimental data, an atomic network model of L1 is proposed [Fig. 2(e)]. The network has the same 2D structure as the SiC surface, but with one-third of the atomic sites being partially occupied by vacancies. A honeycomb structure is built up by Al or Si atoms, where the vacancy sites at the center are surrounded by six Si/Al atoms at each vertex. Viewed from $\langle 10\bar{1}0 \rangle$, as indicated by red arrows in Fig. 2(e), the row of the partial vacancy occupation can be distinguished from that of Si and Al, and consequently, the in-plane ordering is visible. Two Si/Al

rows are shown up as a series of bright-dot pairs, while the rows of partial vacancies are presented as gray dots in the STEM images [Figs. 1(c), 1(e, right), and 1(f)]. Tilted 30° around the normal of the basal plane, those two kinds of rows overlap along $[11\bar{2}0]$, as shown by the blue arrows in Fig. 2(e), and the in-plane ordering is invisible [see Fig. 1(e, left)].

L2 has a similar 2D network with in-plane ordering, visible from the $\langle 10\bar{1}0 \rangle$ direction [see Fig. 1(e, right)]. The slightly reduced intensity of the pairs implies vacancy formation [deep purple spheres in Fig. 2(d)]. Combining the two networks of L1 and L2 together with the adjacent AlN layer and the SiC surface, an opCG-ipVO interface structure is created, which consists of the AlN bottom layer (L3), L2: $(\text{Al}_{2/3}\text{Si}_{1/3})_{1-x}\text{N}$, L1: $(\text{Al}_{1/3}\text{Si}_{2/3})_{2/3+x}\text{N}$, and the SiC substrate surface layer (L0). During the MOCVD process, there was no intentional Si precursor being supplied. Si incorporated in L1 and L2 must thus originate from the SiC substrate surface. Likely, in the initial growth, Al and Si adatoms reacted with N and formed the first intermediate layer L1. The rest of the Si adatoms further reacted with Al and N precursors and formed the second intermediate layer L2 on the top of L1. After the Si adatoms were consumed, the AlN layer started to grow from the L2 surface. Thus, a structural model of the opCG-ipVO interface is proposed in Fig. 2(b).

To clarify the thermodynamic stability of the opCG-ipVO interface, modeling based on density functional theory (DFT) calculations was performed to determine (i) if the formation of ordered vacancies is favored compared to a sharp and perfect interface, (ii) if Si and Al are mixed in L1 and L2, and (iii) if L1 contains C or N in L1 since L1 is Si-rich and next to SiC (details of the code, potential, and computational parameters are given in the supplementary material). In a first step, we investigated if ordered vacancies in L1 are favored as compared to a sharp and perfect interface for models with either C or N in L1. The change in energy for this reaction is given by Eq. S(1). Figure 3(a) (long dashed lines) shows that N in L1 is favored (light blue), while C in L1 is not (orange). The second reaction, using Eq. S(2), includes the mixture of Si and Al in both L1 and L2 for the above given ratios as well as ordered vacancies. The reaction indicates a small increase in energy for both N and C. In the second reaction path, we investigated a mixture of Si and Al in both L1 and L2, for the above given ratios, where the reaction energy is given by Eq. S(3). Figure 3(a) (short dashed lines) shows that N in L1 is favored (light blue), while C in L1 is not favored (orange). This is followed by considering ordered vacancies in L1, with a reaction energy defined from Eq. S(4), which lowers the energy further for N at L1, while the energy increases for C at L1. The results for the two reaction paths shown in Fig. 3(b) indicate that (i) L1 contains N, (ii) a mixture of Si and Al in L1 and L2 is favored, and (iii) the formation of the interface structure with ordered vacancies in L1 is the one most likely to be formed. Figure S3 shows that N in L1 is less sensitive to cell size variations as compared to C in L1. The results presented in Fig. 3(b) are for models with large lateral extension with 27 M sites in layer L2. We have also investigated the chemical distribution of Al and Si in layer L2. For the ordered model, the ordered case is 0.35 eV higher in energy for N in L1 and 0.1 eV lower in energy for C in L1 as seen in Fig. S4. This indicates that there is a

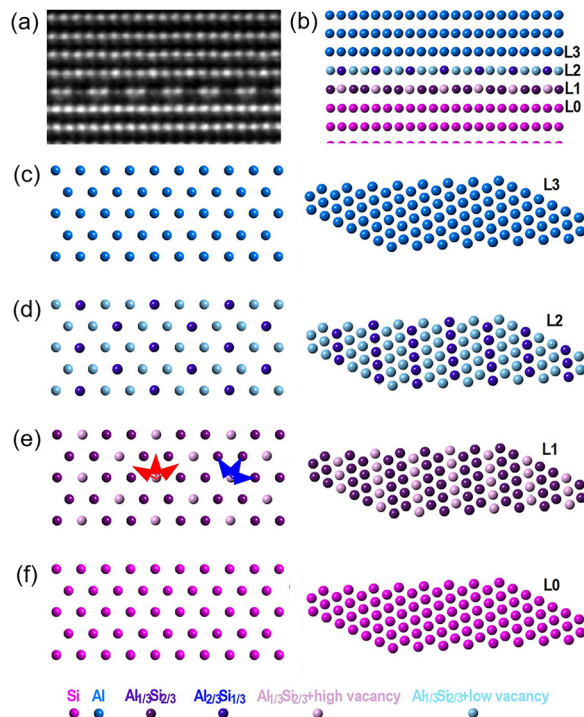


FIG. 2. STEM, structural model of opCG-ipVO, and schematics of 2D networks (a)–(f). STEM image (a), structural model (b), the first layer of AlN: L3 (c), L2 $(\text{Al}_{2/3}\text{Si}_{1/3})_{1-x}\text{N}$ (d), L1 $(\text{Al}_{1/3}\text{Si}_{2/3})_{2/3+x}\text{N}$ (e), and the top layer of SiC: L0 (f), viewed from left: $[0001]$ and right $[11\bar{2}0]$. Note that C and N are too light to give discernible contrast, while Al and Si display almost the same contrast.

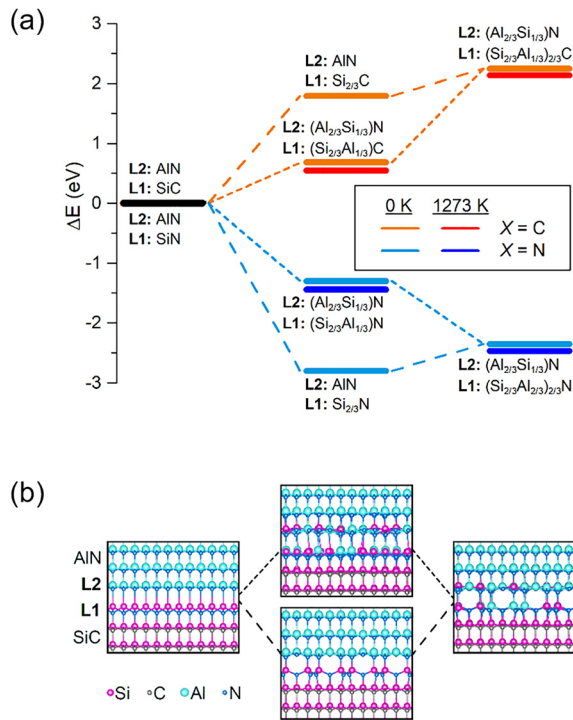


FIG. 3. (a) Calculated energy diagram for different reaction paths going from a sharp interface to an interface with 33% metal vacancies in layer L1 and disorder of Si and Al in layers L1 and L2. (b) Schematics of the interface region, along $[10\bar{1}0]$, for the two reaction paths with N in the L1 layer. Data and schematic structural illustration are from relaxed structural mode with large lateral extension with two- and four-unit cells of SiC and AlN (see Fig. S2), respectively.

preference for a disordered chemical distribution of Al and Si for N, in agreement with our experimental results.

The opCG-ipVO interface provides the intermediate layers L1 and L2, which have similar composition as the SiC substrate and the AlN layer respectively, and the interface mismatch is improved dramatically. Thus, we introduce the term “transmorphic heteroepitaxy,” for which the composition and atomic configuration gradually transit from substratelike to epilayerlike. As a result, the transmorphic epitaxial AlN layer has a low defect density, enabling the growth of a high-quality thin GaN HEMT heterostructure that does not require a conventional thick buffer layer to annihilate the structural defects. The total thickness of the thin GaN HEMT heterostructure is ~ 300 nm, which is 20 times lower than that of the conventional GaN power devices that are qualified for 650 V operation.¹¹

Finally, a thin GaN HEMT heterostructure, like sample A, was grown on a 100 mm semi-insulating 4H-SiC substrate to test the breakdown strength of the high-quality thin epitaxial stack, which nominally consists of 2-nm GaN cap/14-nm $\text{Al}_{0.29}\text{Ga}_{0.71}\text{N}$ barrier layer/0.2- μm GaN channel/60-nm AlN NL. Additionally, Hall measurements performed on Van der Pauw patterns reveal a carrier concentration of $1 \times 10^{13} \text{ cm}^{-2}$ with an electron mobility at room temperature of $2100 \text{ cm}^2/\text{Vs}$, which is comparable to the state-of-the-art transport properties of AlGaN/GaN HEMTs with a conventional thick buffer layer.¹² Lateral breakdown voltage measurements with the

substrate floating (A Keysight B1505A) were conducted on the isolated two-terminal Ohmic contacts with various distances from 5 to 20 μm , as shown in Fig. 4. The device isolation was achieved by nitrogen implantation to locally remove the 2DEG in the volume in between the two contacts to isolate the contacts. The two-terminal device was then immersed in a Fluorinert solution (FC-43) in order to avoid arcing in air¹³ during the measurements. The details of the measurement setup are schematically illustrated in Fig. S5. Quite remarkably, such thin III-nitride epitaxial layers can achieve a breakdown voltage of 1800 V, at the distance of 20 μm . Moreover, a critical breakdown field close to 2 MV/cm was obtained for the short distance of 5 μm , which is well beyond the typical values reported for GaN-based HEMT heterostructures grown on foreign substrates and even higher than that for the GaN devices grown on GaN native substrates.⁵ This is attributed to the presence of the high-quality AlN NL, which virtually serves as a back barrier that enables a critical breakdown field enhancement for the thin GaN layer. This should not be surprising since AlN has the largest critical breakdown field of 11.7 MV/cm among the III-nitrides. For larger contact distances, the electric field spreads deeper within the substrate so that the breakdown may be dominated by the SiC material, which renders a critical breakdown field slightly below 1 MV/cm.¹⁴

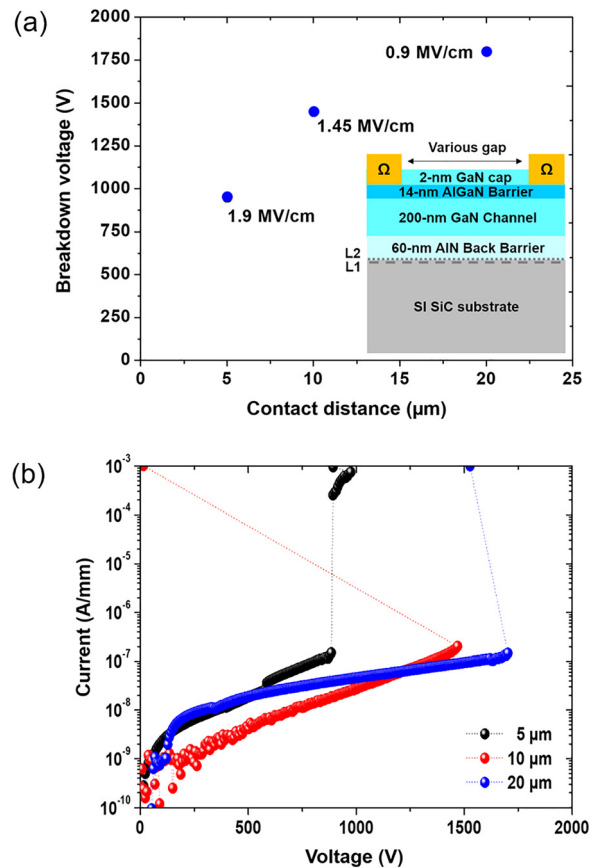


FIG. 4. Lateral breakdown voltage as a function of isolated contact distance (a) and corresponding I-V characteristics (b). The L1 and L2 atomic layers providing transmorphic epitaxial growth of the AlN layer on SiC are indicated by the dashed lines.

Furthermore, no parasitic conduction was observed with a leakage current remaining well-below $1 \mu\text{A}/\text{mm}$ until the breakdown voltage is reached. Additionally, the vertical breakdown of the heterostructure was measured as well. We do not see any breakdown up to 3 kV (not shown here), which is the limit of the setup. This result is consistent with our previous result in Ref. 7, where one can see that there is virtually no breakdown up to 1.5 kV, limited by the delineation of the contact at the time.

In summary, we present a heteroepitaxial growth mode where the interface between the first epitaxial layer and the substrate is mediated by ordered vacancies. Analytical high-resolution STEM shows that a unique interface structure consists of two intermediate atomic layers, one Si-rich and one Al-rich, which define the transmorphous epitaxial growth. With sharing in-plane symmetry and providing a compositional gradient across the intermediate layers to both the epitaxial layer and the substrate, the opCG-ipVO interface significantly alleviates the compositionally induced lattice mismatch and the surface-energy gradient difference between the epitaxial layer and the substrate and consequently results in a high-quality epitaxial AlN nucleation layer, which enables thin GaN HEMT heterostructures grown on the top to exhibit a critical breakdown field of nearly 2 MV/cm. The present work demonstrates that foreign materials have an ability to match each other by modifying the interface structure, which provides a means to grow low-defect-density epitaxial layers in heterosystems. Other variants of compositional gradients and ordering of elements and their vacancies are expected to exist, depending on the processing, as shown by our *ab initio* calculations.

See the [supplementary material](#) for (i) the opCG-ipVO interface over several hundred nanometers, (ii) modeling based on DFT calculations, (iii) the detailed information for structural models, (iv) calculated reaction energies along different reaction paths for two sizes of in-plane and various thicknesses of SiC and AlN, (v) calculated formation energies of the different chemical distribution of Al and Si in layer L2, and (vi) detailed breakdown measurement setup.

J.L. and L.H. acknowledge support to the Linköping Ultra Electron Microscopy Laboratory by the Knut and Alice Wallenberg Foundation Scholar Grant (No. KAW-2016-0358). The calculations were performed using supercomputer resources provided by the Swedish National Infrastructure for Computing (SNIC) at PDC. J.C. and O.K. acknowledge the funding support from the European Union's Horizon 2020 research and innovation programme under

Grant Agreement No. 823260 for the project, CoolHEMT. J.R. acknowledges support from the KAW foundation for a Fellowship Grant and from the Swedish Foundation for Strategic Research for a Framework Grant (No. EM16-0004).

REFERENCES

- J. Wang, J. B. Neaton, H. Zheng, V. Nagarajan, S. B. Ogale, B. Liu, D. Viehland, V. Vaithyanathan, D. G. Schlom, U. V. Waghmare, N. A. Spaldin, K. M. Rabe, M. Wuttig, and R. Ramesh, "Epitaxial BiFeO₃ multiferroic thin film heterostructures," *Science* **299**, 1719–1722 (2003).
- J. W. Orton and C. T. Foxon, "Group III nitride semiconductors for short wavelength light-emitting devices," *Rep. Prog. Phys.* **61**, 1–76 (1998).
- R. Viswanathan, J. A. Zasadzinski, and D. K. Schwartz, "Strained-layer van der Waals epitaxy in a Langmuir-Blodgett film," *Science* **261**, 449–452 (1993).
- H. Amano, N. Sawah, I. Akasaki, and Y. Toyota, "Metalorganic vapor phase epitaxial growth of a high quality GaN film using an AlN buffer layer," *Appl. Phys. Lett.* **48**, 353 (1986).
- J. H. Ng, J. T. Asubar, H. Tokuda, and M. Kuzuhara, "AlGaIn/GaN HEMTs on free-standing GaN substrates with breakdown voltage of 5 kV and effective lateral critical field of 1 MV/cm," in CS ManTech Conference (2016), p. 215.
- S. L. Selvaraj and T. Egawa, "Transmission electron microscopy to study gallium nitride transistors grown on sapphire and silicon substrates," in *The Transmission Electron Microscope*, edited by K. Maaz (InTech, 2012), ISBN: 978-953-51-0450-6.
- J.-T. Chen, J. Bergsten, J. Lu, E. Janzén, M. Thorsell, L. Hultman, N. Rorsman, and O. Kordina, "A GaN-SiC hybrid material for high-frequency and power electronics," *Appl. Phys. Lett.* **113**, 041605 (2018).
- C. Hu, C.-C. Lai, Q. Tao, J. Lu, J. Halim, L. Sun, J. Zhang, J. Yang, B. Anasori, J. Wang, Y. Sakka, L. Hultman, P. Eklund, J. Rosen, and M. W. Barsoum, "Mo₂Ga₂C: A new ternary nanolaminated carbide," *Chem. Commun.* **51**, 6560–6563 (2015).
- G. Kresse and J. Furthmüller, "Efficient iterative schemes for *ab initio* total-energy calculations using a plane-wave basis set," *Phys. Rev. B* **54**, 11169–11186 (1996).
- Y. N. Picard, M. E. Twigg, M. A. Mastro, C. R. Eddy, Jr., R. L. Henry, and R. T. Holm, "Threading dislocation behavior in AlN nucleation layers for GaN growth on 4H-SiC," *Appl. Phys. Lett.* **91**, 014101 (2007).
- H. Amano, Y. Baines, E. Beam, M. Borga, T. Bouchet, P. R. Chalker, M. Charles, K. J. Chen, N. Chowdhury, R. Chu *et al.*, "The 2018 GaN power electronics roadmap," *J. Phys. D* **51**, 163001 (2018).
- J.-T. Chen, I. Persson, D. Nilsson, C.-W. Hsu, J. Palisaitis, U. Forsberg, P. O. Å. Persson, and E. Janzén, "Room-temperature mobility above 2200 cm²/Vs of two-dimensional electron gas in a sharp-interface AlGaIn/GaN heterostructure," *Appl. Phys. Lett.* **106**, 251601 (2015).
- Y. Dora, A. Chakraborty, L. McCarthy, S. Keller, S. P. DenBaars, and U. K. Mishra, "High breakdown voltage achieved on AlGaIn/GaN HEMTs with integrated slant field plates," *IEEE Electron Device Lett.* **27**, 713 (2006).
- M. Noborio and T. Kimoto, "1580-V–40-mΩ·cm² double-RESURF MOSFETs on 4H-SiC (000 $\bar{1}$)," *IEEE Electron Device Lett.* **30**, 831 (2009).